ARTICLE

Molecular Beam Deposition of Nanoscale Ionic Liquids in Ultrahigh Vacuum

Shingo Maruyama,[†] Yoko Takeyama,[†] Hiroki Taniguchi,[†] Hiroki Fukumoto,[‡] Mitsuru Itoh,[†] Hiroshi Kumigashira,[§] Masaharu Oshima,[§] Takakazu Yamamoto,[‡] and Yuji Matsumoto[†,*]

[†]Materials and Structures Laboratory and [‡]Chemical Resources Laboratory, Tokyo Institute of Technology, 4259 Nagatsuta, Midori-ku, Yokohama 226-8503, Japan and [§]Department of Applied Chemistry and JST-CREST, University of Tokyo, Bunkyo-ku, Tokyo 113-8656, Japan

ABSTRACT We propose a new approach to nanoscience and technology for ionic liquids (ILs): molecular beam deposition of IL in ultrahigh vacuum by using a continuous wave infrared (CW-IR) laser deposition technique. This approach has made it possible to prepare a variety of "nano-IL" with the given composition on the substrate: a nanodroplet, on one hand, the volume of which goes down to 1 aL and, on the other hand, an ultrathin film with a thickness to several 100 nm or less. The result of fractional distillation of a binary mixture of ILs, investigated by nuclear magnetic resonance as well as electrospray ionization time-of-flight mass spectrometry, indicates that this deposition process is based on the thermal evaporation of ILs, and thus this process also can be used as a new purification method of ILs in vacuum. Furthermore, the fabrication of binary mixture droplets of two ILs on the substrate by alternating deposition of two ILs was demonstrated; the homogeneity of the composition was confirmed even for one single droplet by high-spatial-resolution Raman spectroscopy.

KEYWORDS: ionic liquids · CW-IR laser deposition · nanodroplets · liquid thin film · fractional distillation

Ionic liquids (ILs) are attracting many researchers as a new nonvolatile liquid solvent for organic synthesis,[1,2] catalytic media,[3] electrochemistry,[4] solar cells,[5,6] fuel cells,[7,8] and so on. Their ultimate low vapor pressure has allowed us to open a new research field of ILs to materials characterization and processing in vacuum. However, most of the studies of ILs in vacuum are concerned with "bulk" ILs, which may become an obstacle in the way of their further applications to nanoscience and technology. Thus a sophisticated nanopreparation technique in vacuum would be highly required for precisely controlled thin films and droplets of ILs on a substrate, as an analogy of solid-state physics and semiconductor technology, associated with using powerful vacuum deposition techniques, such as molecular beam epitaxy. Here, we have established an excellent method of molecular beam deposition for nanoscale ILs in forms, such as droplets and thin films, by using a continuous wave infrared (CW-IR) laser deposition technique.[9]

Such nanoscale liquid droplets and thin films are getting a growing importance in basic science and engineering. As an example, physics of the liquids droplet at the nanoscale is an attractive subject in terms of a size effect of their physical properties, such as surface tension,[10] while the thin film of liquid, as another example, still has some important applications, such as a lubricant.[11] Negligible vapor pressure of ILs is a favorable feature as a model system because high-vacuum analytical techniques, such as scanning electron microscope (SEM)[12,13] and photoelectron spectroscopy,[14−16] become available for their surface characterizations. On the other hand, Earle *et al.*[17] reported some ILs could be distilled without decomposition in vacuum. This result encourages us to prepare in vacuum IL samples whose composition and amount are precisely controlled. As for the related previous works, there are some reports on the volatility of IL[18−22] and gas-phase studies.[23−28] However, information about the resultant condensed ILs on the substrate after the vaporization is scarce. Cremer *et al.*[29] reported the physical vapor deposition of ILs on a glass substrate by heating an IL in a gold reservoir in vacuum. They, from the X-ray photoelectron spectroscopy (XPS) measurement, claimed that two-dimensional growth of an IL molecular layer was found in the beginning of deposition. Recently, Sobota *et al.*[30] applied infrared reflection absorption spectroscopy (IRAS), together with density functional theory (DFT) calculation, to investigate the orientation of IL molecule on a well-ordered alumina surface deposited by an ultrahigh vacuum (UHV) compatible evaporator. There are some other approaches to prepare nanoscale droplets or

*Address correspondence to matsumoto.y.ad@m.titech.ac.jp.

Received for review May 12, 2010 and accepted September 16, 2010.

Published online September 23, 2010. 10.1021/nn101036v

© 2010 American Chemical Society

thin films of IL, such as evaporation of methanol from an IL-methanol solution[31,32] or a nanoinkjet printing method.[33] With these backgrounds, we have established a new molecular beam deposition method to serve nanoscale ILs using a CW-IR laser deposition technique. The CW-IR laser deposition is similar to that originally developed in our group for precise-controlled deposition of π-conjugated compounds.[9]

RESULT AND DISCUSSION

Figure 1a shows an experimental setup. Vacuum deposition was carried out at room temperature using a standard UHV chamber with a base pressure of ~3 × 10^{-9} torr. An 808 nm CW-IR laser beam was introduced into the chamber through a quartz window and irradiated to the IL. A Si powder was added to the IL in the container, for efficient absorption of the IR laser, because most ILs are transparent to this wavelength. The CW-IR laser was modulated into 10−30 ms pulses with a repetition frequency of 2 or 4 Hz. Controllability of the deposition amount was checked by a quartz crystal microbalance (QCM) during deposition.

Laser power density in this experiment ranged from 260 to 390 W/cm^2. The kind of ILs can be selected by rotating a target holder. In this deposition system, an *in situ* UHV laser microscope (LM) is available to observe the morphology, and thermal behavior of ILs is deposited on the substrate without air exposure. Figure 1b shows a typical UHV-LM image of 1-butyl-3-methylimidazolium bis(trifluoromethanesulfonyl)imide ([bmim][NTf_2]) droplets deposited on a sapphire substrate. These microdroplets were stable for more than several hours in vacuum and vaporized at temperatures above 450 K at 5 × 10^{-7} torr (See Supporting Information, video and Figure S1).

Precise control of the deposition amount is important for making nanoscale droplets or thin films by alternate deposition, as described below. We examined the effects of Si powder and pulse modulation of the CW-IR laser on the controllability in the deposition. Figure 2 shows a data set of the mass change with time, monitored by QCM, during the deposition under different conditions. In the case of (a), *i.e.*, when the continuous laser is irradiated to the pure IL target, the initial deposition rate is very low, and it suddenly increases as a function of heating time. This is because the IL container has a relatively large heat capacity to absorb the IR laser so that it takes a long time for the container itself to heat up, and consequently undesired deposition continues even after turning off the laser. On the other hand, in the case of (b) when the pulsed laser is used instead, it does not work at all; almost no deposition occurs because the net heating power is quite low. If we put the Si powder into the IL target and irradiate it with the continuous laser, as in the case of (c), the IR absorption becomes more effective so that the deposition

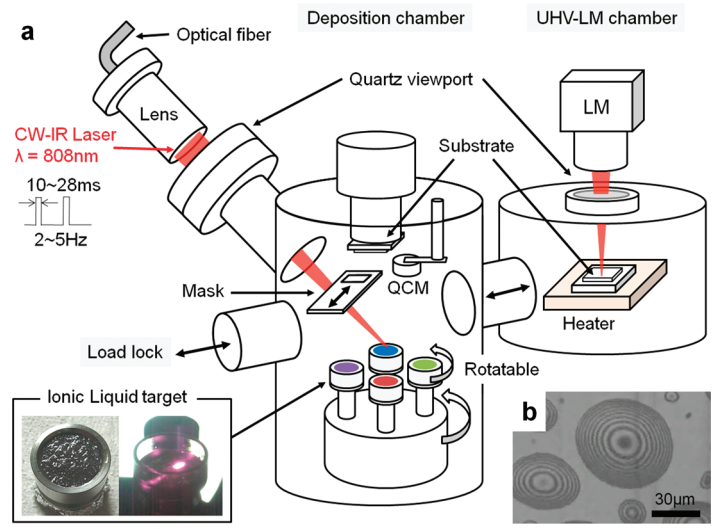

Figure 1. Experimental setup. (a) A schematic of the CW-IR laser deposition of ionic liquids with a UHV-LM. (b) An *in situ* LM image of the deposited [bmim][NTf_2] droplets on a sapphire substrate at 445 K in 4 × 10^{-7} torr.

starts upon IR irradiation and stops quickly by turning off the laser, although the deposition rate gradually increases in the meanwhile. In the last case of (d), that the pulsed laser is used instead with the Si powder, the constant deposition rate as well as a clear response to laser switching is attained. In the present study, we optimized the weight ratio of Si powder in the IL target to be about 60% so as to precisely control the amount of the deposited IL on nanoscale (Supporting Information,

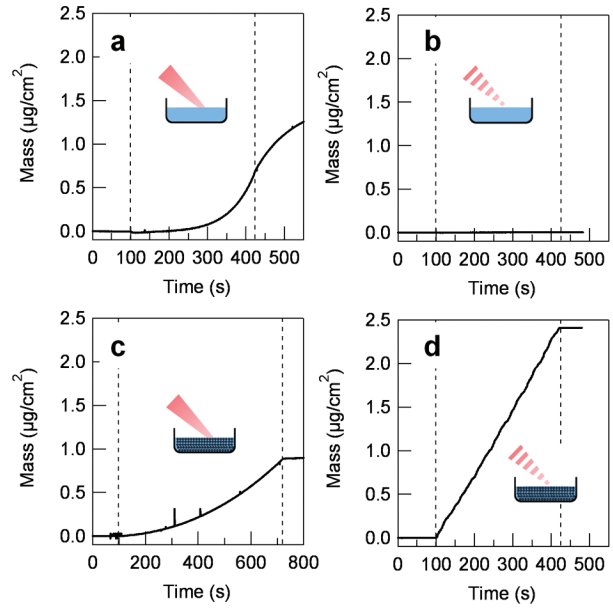

Figure 2. Comparison of controllability in the CW-IR laser deposition of [bmim][NTf_2] by using QCM. (a) Without Si powder, continuous irradiation (80 W/cm^2 power density). (b) Without Si powder, pulsed irradiation (10 ms pulse width, 2 Hz repetition frequency, and 260 W/cm^2 power density). (c) With Si powder, continuous irradiation (26 W/cm^2 power density). (d)With Si powder, pulsed irradiation (10 ms pulse width, 2 Hz repetition frequency, and 260 W/cm^2 power density).

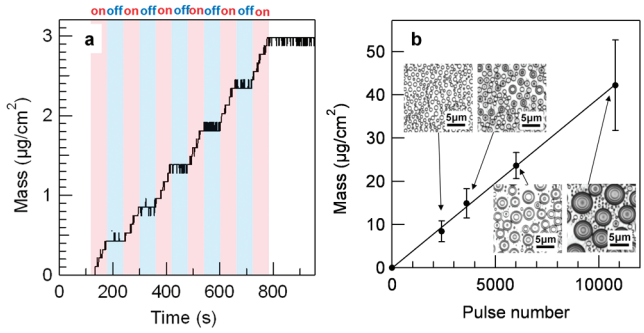

Figure 3. Precise control of deposition amount by using CW-IR laser deposition technique. (a) Digital control of deposition amount of [bmim][NTf$_2$] monitored by QCM (laser pulse width = 10 ms, repetition frequency = 2 Hz, and power density = 260 W/cm^2). (b) Mass of [bmim][NTf$_2$] on a sapphire substrate estimated by laser microscope images, and there is a good linear relationship between the deposition amount and the pulse number.

Figure S2). Based on these preliminary experiments, we demonstrated digital control of stable IL deposition with a clear response of the deposition to on−off switching of the pulsed CW-IR laser, when used the Si powder as an absorbent of the laser as shown in Figure 3a. The deposition rate could be controlled to be as low as 0.03 μg/cm^2/s (= 0.02 pL/cm^2/s), and it was stable for a long-term deposition, up to the deposition amount of 40 μg/cm^2 (= 28 μL/cm^2) as is measured by the *ex situ* LM (Figure 3b).

Stability of ILs during the deposition was examined using the deposited IL on a glass, which was characterized by ^{1}H, ^{19}F, and ^{31}P nuclear magnetic resonance (NMR) spectroscopy and electrospray ionization time-of-flight mass spectrometry (ESI-TOF-MS) (Supporting Information Figures S3−S17). The ^{1}H NMR data (Table 1) revealed that [PC$_{66614}$][NTf$_2$] could be successfully deposited without significant decomposition in UHV and [hmim][OTf] also even in 1 torr O_2, although these ILs are ready to decompose when distilled with continuous heating at 300 °C in low vacuum conditions by using a Kugelrohr oven.[17] At present, there are two possible reasons why the CW-IR laser deposition did not cause significant decomposition for these ILs. The first one is that the instantaneous laser pulse heats only a region near the surface of IL, and thus the heat damage to ILs would be minimized. The second one is that the vaporization of ILs in this process may occur at temperatures much lower than that of the decomposition temperatures of ILs because of the ultrahigh vacuum condition. In fact, in order to directly measure the actual temperature of IL target samples during the CW-IR laser irradiation, we employed a pyrometer (Japan Sensor, FTZ2-R) that can measure the temperature in a smaller spot diameter (~2 mm) than the CW-IR laser beam spot on the IL sample with a shorter acquisition time (1 ms) than the CW IR laser pulse width (10 ms). The temperature on the target sample of [bmim][NTf$_2$] with Si powder irradiated by CW-IR laser (pulse width = 10 ms, pulse period = 250 ms, and power = 260W/cm^2) was around 350 °C. This temperature is much lower than the reported thermal decomposition temperature of [bmim][NTf$_2$], 427 °C estimated by a thermogravimetric analysis in N_2 atmosphere.[34] In the process of IL deposition, the Si powder works just as an absorbent of IR laser without evaporation, because Si evaporates at much higher temperatures than the temperature of IL decomposition. It was confirmed from our X-ray photoemission spectroscopy study within the detection limit that no sign of Si was included in the [bmim][NTf$_2$] deposited on a conductive Nb-doped $SrTiO_3$ substrate (not shown).

The present CW-IR deposition method is basically based on the thermal evaporation of ILs, consequently fractional distillation and purification of thermally unstable ILs, which easily decompose in the conventional distillation, are expected to become possible by using the present method. In fact, when an approximately equimolar mixture target of [bmim][NTf$_2$] and [bmim][PF$_6$] was used to deposit, the [bmim][PF$_6$] mole fraction in the deposited IL became smaller than 6%, as determined by ^{19}F NMR spectroscopy (Figure 4 a and b). We also confirmed this result by using ESI-TOF-MS: the mixture target and the deposit sample were extracted by acetonitrile, and ESI-TOF-MS spectra of the extracts were measured under negative mode conditions (inset of Figure 4). The anionic peaks at m/z = 145 and 280 correspond to [PF$_6$]$^-$ and [NTf$_2$]$^-$, respectively. The peak intensity of [PF$_6$]$^-$ in the spectrum of the as-deposited sample (the inset of Figure 4b) was very weak to that of [NTf$_2$]$^-$, indicating that [bmim][NTf$_2$]

TABLE 1. Deposition Condition and Fraction of Decomposition in the Deposited IL Estimated by ^{1}H NMR

ionic liquid	ambient (torr)	frequency (Hz)	pulse width (ms)	laser power (W/cm^2)	deposition time (h)	fraction of decomposition in deposited IL(%)
[emim][NTf$_2$]	4×10^{-8}	4	14	340	11.5	<1
[bmim][NTf$_2$]	3×10^{-8}	4	10	260	39.5	<1
[bmim][PF$_6$]	2×10^{-8}	4	14	340	30	<1
[bmim][BF$_4$]	1×10^{-8}	4	10	260	72	<1
[PC$_{66614}$][NTf$_2$]	8×10^{-7}	4	14	260	6.5	<1
[hmim][OTf]	1×10^{-8}	4	22	340	12	<1
[hmim][OTf]	1 (O_2)	4	28	340	7.4	<1
[emim][EtSO$_4$]	6×10^{-6}	4	28	390	6	<10

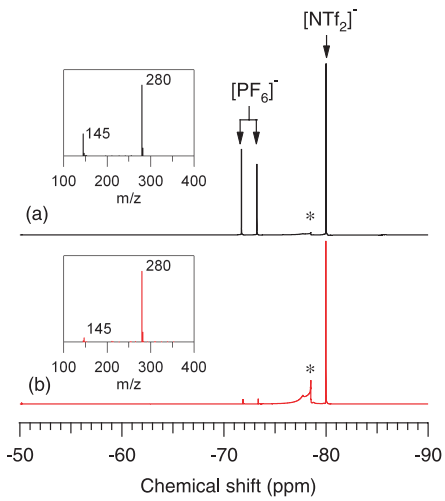

Figure 4. ^{19}F NMR (470.40 MHz, acetone-d_6, external standard CF_3COOH = −78.5 ppm marked with asterisk) spectra of mixture target of [bmim][NTf_2] and [bmim][PF_6] and as-deposited sample in vacuum. Mixture target was irradiated by CW-IR laser at 15 ms pulse width, 4 Hz repetition rate, and 260 W/cm^2 power density. From the value of integral of the peaks, the molar fratio of [bmim][NTf_2] and [bmim][PF_6] in a mixture target was approximately equal (a) and the [bmim][PF_6] mole fraction in the deposited IL was smaller than 6% (b). Inset shows anionic mass spectra of the corresponding mixture target and deposited sample. The anionic peaks at m/z = 145 and 280 were assigned to $[PF_6]^-$ and $[NTf_2]^-$, respectively. The intensity ratio of $[PF_6]^-$ to $[NTf_2]^-$ was clearly found to decrease after the deposition.

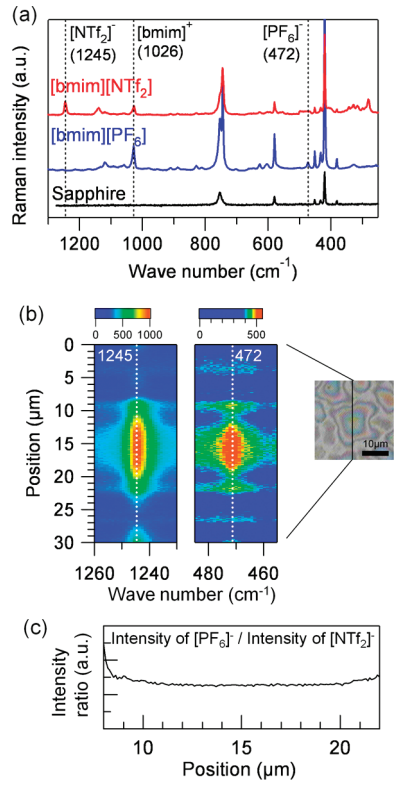

Figure 5. A set of Raman spectra for the deposited [bmim][NTf_2] and [bmim][PF_6] on a sapphire substrate. The peaks at 1026, 1245, and 472 cm^{-1} which are assigned to $[bmim]^+$, $[NTf_2]^-$ and $[PF_6]^-$ ions, respectively. (b) The peak intensities at 1245 ($[NTf_2]^-$) and 472 cm^{-1} ($[PF_6]^-$) in line scanned Raman spectra were mapped out along the cross-sectional line indicated in the corresponding optical image of an isolated IL droplet. (c) The variation of the intensity ratio of $[PF_6]^-$ (472) to $[NTf_2]^-$ (1245 cm^{-1}) along the scanned line.

was essentially deposited, and it is well consistent with the result of ^{19}F NMR. These results are, on one hand, well consistent with the reported results,[24] but on the other hand, suggest that preparation of a binary system of these ILs is difficult by this technique from the corresponding mixed ILs target. However, the present CW-IR deposition method makes it possible to prepare such a binary system of [bmim][NTf_2] and [bmim][PF_6] ILs with the given composition, by taking advantage of using the nanoscale deposition: an alternating deposition of two ILs by switching the target. The mass of one cycle deposition is about 0.24 μg/cm^2 (= 0.17 pL/cm^2) with a deposition rate of 0.03 μg/cm^2/s (= 0.02 pL/cm^2/s). After 23 times reputation, we get about 5.6 μg/cm^2 (= 3.9 pL/cm^2) ILs on a substrate. Within one cycle the deposited amount seems to be small enough to ensure the complete mixing. A set of Raman spectra for the deposited [bmim][NTf_2] and [bmim][PF_6] on a sapphire substrate is first shown in Figure 5a, together with that of the sapphire substrate itself as a reference. The peaks observed at 1026, 1245, and 472 cm^{-1} are assigned to $[bmim]^+$, $[NTf_2]^-$, and $[PF_6]^-$ ions, respectively, from previous reports.[35,36] As shown in Figure 5b, for an isolated droplet along the cross-sectional line indicated in the corresponding optical image, the peak intensities at 1245 ($[NTf_2]^-$) and 472 cm^{-1} ($[PF_6]^-$), in line scanned Raman spectra were traced. Figure 5c displays the variation of the intensity ratio of $[PF_6]^-$ (472) to $[NTf_2]^-$ (1245 cm^{-1}) along the scanned line shown in Figure 5b. The intensity ratio was almost constant over the droplet, indicating that both ILs were homogeneously mixed within the resolution limit of line scanned Raman spectra. The present preparation method of ILs mixture would be of great benefit to us in search of better combination or composition of ILs for various applications.

Finally, a set of SEM and tapping mode atomic force microscopy (AFM) topographic images of [bmim][PF_6]/sapphire(0001) and [omim][NTf_2]/Si(100), respectively, is shown in Figure 6. Micro- and submicrometer IL droplets with a contact angle of about 20° are clearly seen (Figure 6a and b) in the case of [bmim][PF_6] deposited on the sapphire(0001) substrate. The volume of one droplet reaches as small as 1 aL. The size of these small droplets of IL is well controlled by changing deposition time, as discussed above. For example, for the three IL samples of [emim][NTf_2] on a sapphire(0001) substrate prepared under almost the same deposition conditions, the diameter distribution of IL droplets seems reproducible: the average size is 1.8 μm with

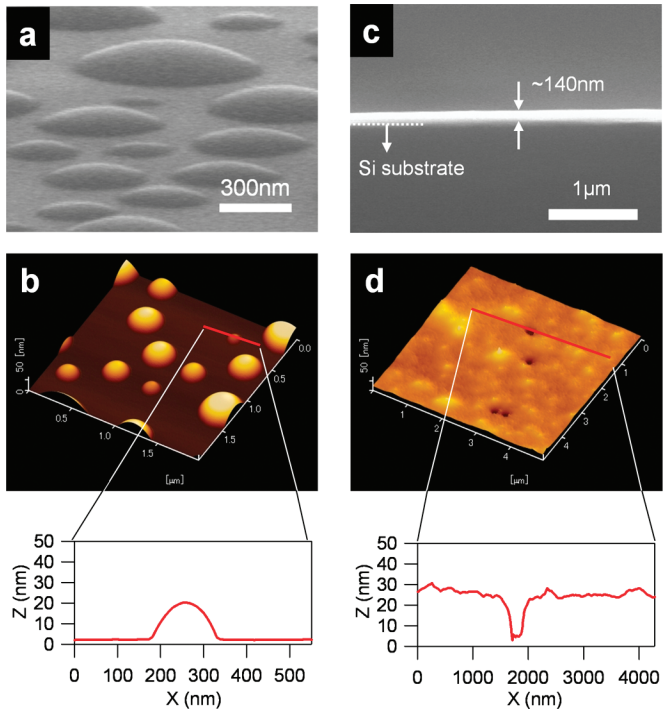

Figure 6. A set of SEM and tapping-mode AFM topographic images, together with their line profiles of [bmim][PF_6] on a sapphire(0001) substrate (a and b) and [omim][NTf_2] with C_{60} seed layer on a Si(100) substrate (c and d).

a standard deviation of 0.7 μm (Supporting Information, Figure S18 and Table S1), though the size of IL droplets on the substrate crucially depends on the surface condition of the substrate. In contrast, with a 5 nm C_{60} seed layer, the wettability of [omim][NTf_2] on the substrate is much improved compared to the case without the seed layer (Supporting Information, Figure S19), and an almost completely wetting ultrathin film of [omim][NTf_2] is obtained (Figure 6c and d). Generally, an increase of the surface area having a good affinity to a certain liquid leads to improvement in its wettability.[37] In the present case, a sizable amount of C_{60} can dissolve into [omim][NTf_2], suggestive of its better chemical affinity to [omim][NTf_2], as compared to other imidazolium ILs.[38] Thus, the C_{60} seed layer has a good affinity to the [omim][NTf_2], and the increase of the surface area of C_{60} by being rough might improve the wettability of [omim][NTf_2]. These droplets and thin film are very stable for several weeks in air, suitable to further material processes with them and their characterizations.

SUMMARY

By using a continuous wave infrared (CW-IR) laser deposition system compatible to the conventional ultrahigh vacuum (UHV) processes, successful deposition of nanoscale ionic liquids (ILs), such as droplets and thin films, was demonstrated. Nuclear magnetic resonance (NMR) and electrospray ionization time-of-flight mass spectrometry (ESI-TOF-MS) results revealed that no significant decomposition occurs through deposition and that fractional distillation of ILs binary mixture is also possible. Furthermore, nanoscale alternating deposition of two ILs enables to prepare homogeneously mixed IL droplets on a substrate with designed composition. This new technique allows us not only to accelerate the existing various studies on ILs in vacuum but also opens a door to a great many possibilities for new nanoscience and technology of ILs.

METHODS

Chemicals. 1-Butyl-3-methylimidazolium bis(trifluoromethylsulfonyl)amide ([bmim][NTf_2]) and 1-butyl-3-methylimidazolium hexafluorophosphate ([bmim][PF_6]) were purchased from Kanto Kagaku. 1-Ethyl-3-methylimidazolium bis(trifluoromethylsulfonyl)amide ([emim][NTf_2]), 1-butyl-3-methylimidazolium tetrafluoroborate ([bmim][BF_4]), and 1-ethyl-3-methylimidazolium ethylsulfate ([emim][$EtSO_4$]) were purchased from Tokyo Kasei. Trihexyltetradecylphosphonium bis(trifluoromethylsulfonyl)amide ([PC_{66614}][NTf_2]) and 1-hexyl-3-methylimidazolium trifluoromethanesulfonate ([hmim][OTf]) were purchased from Sigma-Aldrich. All ionic liquids were used without further purification.

Instruments. The monitoring the deposition rate of ILs with QCM (Figures 2 and 3) and their evaporation behavior observed by UHV-LM (Figure 1b and Supporting Information, Figure S2) are *in situ*, others such as NMR, Raman, conventional LM, AFM, SEM, and ESI-TOF-MS are *ex situ*. A fiber-coupled diode laser from LIMO (model LDD50, 808 nm) was used for CW-IR laser deposition. Originally developed UHV-LM[39] (Lasertech) was used to observe the evaporation process of IL droplets in vacuum. Keyence VK-8510 was used to estimate the volume of IL deposited on a substrate. NMR spectra were measured on JEOL NMR400. ESI-TOF-MS spectra were obtained by Bruker Daltonics micrOTOF II. Before ESI-TOF-MS measurement, samples are dissolved in acetonitrile. AFM images were measured on Seiko Instruments SPA-400. SEM images were measured on Hitachi S-4000 at acceleration voltage of 20 kV. For the Raman spectroscopy measurements, an incident laser of 532 nm was focused onto the sample with an objective lens (N.A. = 0.7), where the irradiated power was around 15mW on sample. A scattered light was collected by the same objective lens with a back scattering geometry and analyzed by a Jobin Yvon HR-320 single monochromator after filtering by a confocal slit. Raman spectra were finally acquired by a liquid N_2 cooled charge coupled device (CCD) camera. A frequency resolution of the present setup attains about 1.5 cm^{-1}. A line scanning observation was performed by a high-resolution stepping motor stage (SIGMA TECH FX-1100XY) with an interval of 100 nm for one step, where the spatial position was precisely controlled by a closed-loop control. The lateral spatial resolution used for this measurement is as high as 500 nm.

Fabrication of the IL Thin Film. A C_{60} thin film, as a seed layer to improve wettability of IL, was deposited by the CW-IR laser deposition technique on a Si substrate with 250 ms pulse width, 2 Hz repetition frequency, and ~1W/cm^2 laser power in ~3 × 10^{-8} torr. After the deposition of C_{60}, [omim][NTf_2] was then deposited with 10 ms pulse width, 4 Hz repetition frequency, and ~260 W/cm^2 laser power in ~5 × 10^{-9} torr.

Acknowledgment. This work was partially supported by a Research Grant Program from New Energy and Industrial Technol-

ogy Development Organization (NEDO) of Japan. We thank Center for Advanced Materials Analysis (Suzukakedai), Technical Department, Tokyo Institute of Technology for ESI-TOF-MS measurement. S.M. thanks Tokyo Institute of Technology Global COE Program.

Note Added after ASAP Publication: This article was published ASAP on September 23, 2010, with incorrect information in the caption for Figure 2c. The correct version was reposted on September 28, 2010.

Supporting Information Available: ^{1}H, ^{19}F, ^{31}P NMR and ESI-TOF-MS spectra of deposited ILs which are not included in the main text. SEM and AFM image of [omim][NTf_2] droplets on the Si substrate without C_{60} seed layer. Evaporation behavior of deposited [bmim][NTf_2] on a sapphire substrate in 5×10^{-7} torr observed by UHV-LM. This material is available free of charge *via* the Internet at http://pubs.acs.org.

REFERENCES AND NOTES

1. Welton, T. Room-Temperature Ionic Liquids. Solvents for Synthesis and Catalysis. *Chem. Rev.* **1999**, *99*, 2071–2084.
2. Wasserscheid, P.; Welton, T. *Ionic Liquids in Synthesis*; Wiley-VCH Verlag GMBH & Co. KGaA: Weinheim, Germany 2007.
3. Welton, T. Ionic Liquids in Catalysis. *Coord. Chem. Rev.* **2004**, *248*, 2459–2477.
4. *Electrochemical Aspects of Ionic Liquids*; Ohno, H., Ed.; Wiley-Interscience: NJ, 2005.
5. Bonhôte, P.; Dias, A.-P.; Papageorgiou, N.; Kalyanasundaram, K.; Grätzel, M. Hydrophobic, Highly Conductive Ambient-Temperature Molten Salts. *Inorg. Chem.* **1998**, *35*, 1168–1178.
6. Bai, Y.; Cao, Y.; Zhang, J.; Wang, M.; Li, R.; Wang, P.; Zakeeruddin, S. M.; Grätzel, M. High-performance Dye-sensitized Solar Cells Based on Solvent-Free Electrolytes Produced from Eutectic Melts. *Nat. Mater.* **2008**, *7*, 626–630.
7. Noda, A.; Susan, A. B.; Kudo, K.; Mitsushima, S.; Hayamizu, K.; Watanabe, M. Bronsted Acid-base Ionic Liquids as Proton-Conducting Nonaqueous Electrolytes. *J. Phys. Chem. B* **2003**, *107*, 4024–4033.
8. Nakamoto, H.; Noda, A.; Hayamizu, K.; Hayashi, S.; Hamaguchi, H.; Watanabe, M. Proton-Conducting Properties of a Brønsted Acid-Base Ionic Liquid and Ionic Melts Consisting of Bis(trifluoromethanesulfonyl)imide and Benzimidazole for Fuel Cell Electrolytes. *J. Phys. Chem. C* **2007**, *111*, 1541–1548.
9. Yaginuma, S.; Itaka, K.; Haemori, M.; Katayama, M.; Ueno, K.; Ohnishi, T.; Lippmaa, M.; Matsumoto, Y.; Koinuma, H. Molecular Layer-by-Layer Growth of C_{60} Thin Films by Continuous-Wave Infrared Laser Deposition. *Appl. Phys. Exp.* **2008**, *1*, 015005.
10. Checco, A.; Guenoun, P.; Daillant, J. Nonlinear Dependence of the Contact Angle of Nanodroplets on Contact Line Curvature. *Phys. Rev. Lett.* **2003**, *91*, 186101.
11. Kamimura, H.; Kubo, T.; Minami, I.; Mori, S. Effect and Mechanism of Additives for Ionic Liquids as New Lubricants. *Tribol. Int.* **2007**, *40*, 620–625.
12. Kuwabata, S.; Kongkanand, A.; Oyamatsu, D.; Torimoto, T. Observation of Ionic Liquid by Scanning Electron Microscope. *Chem. Lett.* **2006**, *35*, 600–601.
13. Arimoto, S.; Oyamatsu, D.; Torimoto, T.; Kuwabata, S. Development of *In Situ* Electrochemical Scanning Electron Microscopy with Ionic Liquids as Electrolytes. *ChemPhysChem* **2008**, *9*, 763–767.
14. Hofft, O.; Bahr, S.; Himmerlich, M.; Krischok, S.; Schaefer, J. A.; Kempter, V. Electronic Structure of the Surface of the Ionic Liquid [EMIM][Tf_2N] Studied by Metastable Impact Electron Spectroscopy (MIES), UPS, and XPS. *Langmuir* **2006**, *22*, 7120–7123.
15. Smith, E. F.; Rutten, F. J. M.; Villar-Garcia, I. J.; Briggs, D.; Licence, P. Ionic Liquids in Vacuo: Analysis of Liquid Surfaces Using Ultra-High-Vacuum Techniques. *Langmuir* **2006**, *22*, 9386–9392.
16. Kolbeck, C.; Cremer, T.; Lovelock, K. R. J.; Paape, N.; Schulz, P. S.; Wasserscheid, P.; Maier, F.; Steinruck, H. P. Influence of Different Anions on the Surface Composition of Ionic Liquids Studied Using ARXPS. *J. Phys. Chem. B* **2009**, *113*, 8682–8688.
17. Earle, M. J.; Esperança, J. M. S. S.; Gilea, M. a.; Lopes, J. N. C.; Rebelo, L. P. N.; Magee, J. W.; Seddon, K. R.; Widegren, J. a. The Distillation and Volatility of Ionic Liquids. *Nature* **2006**, *439*, 831–834.
18. Esperanca, J. M. S. S.; Lopes, J. N. C.; Tariq, M.; Santos, L. M. N. B. F.; Magee, J. W.; Rebelo, L. P. N. Volatility of Aprotic Ionic Liquids - A Review. *J. Chem. Eng. Data* **2010**, *55*, 3–12.
19. Zaitsau, D. H.; Kabo, G. J.; Strechan, A. A.; Paulechka, Y. U.; Tschersich, A.; Verevkin, S. P.; Heintz, A. Experimental Vapor Pressures of 1-alkyl-3-methylimidazolium Bis(Trifluoromethylsulfonyl)Imides and a Correlation Scheme for Estimation of Vaporization Enthalpies of Ionic Liquids. *J. Phys. Chem. A* **2006**, *110*, 7303–7306.
20. Paulechka, Y. U.; Zaitsau, D. H.; Kabo, G. J.; Strechan, A. A. Vapor Pressure and Thermal Stability of Ionic Liquid 1-butyl-3-methylimidazolium Bis(Trifluoromethylsulfonyl)amide. *Thermochim. Acta* **2005**, *439*, 158–160.
21. Armstrong, J. P.; Hurst, C.; Jones, R. G.; Licence, P.; Lovelock, K. R. J.; Satterley, C. J.; Villar-Garcia, I. J. Vapourisation of Ionic Liquids. *Phys. Chem. Chem. Phys.* **2007**, *9*, 982–990.
22. Taylor, A. W.; Lovelock, K. R. J.; Deyko, A.; Licence, P.; Jones, R. G. High Vacuum Distillation of Ionic Liquids and Separation of Ionic Liquid Mixtures. *Phys. Chem. Chem. Phys.* **2010**, *12*, 1772–1783.
23. Dessiaterik, Y.; Baer, T.; Miller, R. E. Laser Ablation of Imidazolium Based Ionic Liquids. *J. Phys. Chem. A* **2006**, *110*, 1500–1505.
24. Leal, J. P.; Esperança, J. M. S. S.; da Piedade, M. E. M.; Lopes, J. N. C.; Rebelo, L. P. N.; Seddon, K. R. The Nature of Ionic Liquids in the Gas Phase. *J. Phys. Chem. A* **2007**, *111*, 6176–6182.
25. Akai, N.; Parazs, D.; Kawai, A.; Shibuya, K. Cryogenic Neon Matrix-Isolation FTIR Spectroscopy of Evaporated Ionic Liquids: Geometrical Structure of Cation-Anion 1:1 Pair in the Gas Phase. *J. Phys. Chem. B* **2009**, *113*, 4756–4762.
26. Strasser, D.; Goulay, F.; Kelkar, M. S.; Maginn, E. J.; Leone, S. R. Photoelectron Spectrum of Isolated Ion-Pairs in Ionic Liquid Vapor. *J. Phys. Chem. A* **2007**, *111*, 3191–3195.
27. Strasser, D.; Goulay, F.; Belau, L.; Kostko, O.; Koh, C.; Chambreau, S. D.; Vaghjiani, G. L.; Ahmed, M.; Leone, S. R. Tunable Wavelength Soft Photoionization of Ionic Liquid Vapors. *J. Phys. Chem. A* **2010**, *114*, 879–883.
28. Chambreau, S. D.; Vaghjiani, G. L.; To, A.; Koh, C.; Strasser, D.; Kostko, O.; Leone, S. R. Heats of Vaporization of Room Temperature Ionic Liquids by Tunable Vacuum Ultraviolet Photoionization. *J. Phys. Chem. B* **2010**, *114*, 1361–1367.
29. Cremer, T.; Killian, M.; Gottfried, J. M.; Paape, N.; Wasserscheid, P.; Maier, F.; Steinrück, H.-P. Physical Vapor Deposition of [EMIM][Tf_2N]: A New Approach to the Modification of Surface Properties with Ultrathin Ionic Liquid Films. *ChemPhysChem* **2008**, *9*, 2185–2190.
30. Sobota, M.; Nikiforidis, I.; Hieringer, W.; Paape, N.; Happel, M.; Steinruck, H. P.; Gorling, A.; Wasserscheid, P.; Laurin, M.; Libuda, J. Toward Ionic-Liquid-Based Model Catalysis: Growth, Orientation, Conformation, and Interaction Mechanism of the $[Tf_2N]^-$ Anion in [BMIM][Tf_2N] Thin Films on a Well-Ordered Alumina Surface. *Langmuir* **2010**, *26*, 7199–7207.
31. Liu, Y. D.; Zhang, Y.; Wu, G. Z.; Hu, J. Coexistence of Liquid and Solid Phases of Bmim-PF_6 Ionic Liquid on Mica Surfaces at Room Temperature. *J. Am. Chem. Soc.* **2006**, *128*, 7456–7457.
32. Bovio, S.; Podesta, A.; Lenardi, C.; Milani, P. Evidence of Extended Solidlike Layering in [Bmim][NTf_2] Ionic Liquid Thin Films at Room-Temperature. *J. Phys. Chem. B* **2009**, *113*, 6600–6603.

33. Kaisei, K.; Kobayashi, K.; Matsushige, K.; Yamada, H. Ionic Liquid Thin Film Fabrication Using Nano-Inkjet Printing Method. *Jpn. J. Appl. Phys.* **2010**, *49*, 06GH02.
34. Tokuda, H.; Hayamizu, K.; Ishii, K.; Susan, M. A. B. H.; Watanabe, M. Physicochemical Properties and Structures of Room Temperature Ionic Liquids. 2. Variation of Alkyl Chain Length in Imidazolium Cation. *J. Phys. Chem. B* **2005**, *109*, 6103–6110.
35. Rey, I.; Johansson, P.; Lindgren, J.; Lassegues, J. C.; Grondin, J.; Servant, L. Spectroscopic and Theoretical Study of $(CF_3SO_2)_2N^-$ ($TFSI^-$) and $(CF_3SO_2)_2$ NH (HTFSI). *J. Phys. Chem. A* **1998**, *102*, 3249–3258.
36. Talaty, E. R.; Raja, S.; Storhaug, V. J.; Dolle, A.; Carper, W. R. Raman and Infrared Spectra and a Initio Calculations of C_{2-4}MIM Imidazolium Hexafluorophosphate Ionic Liquids. *J. Phys. Chem. B* **2004**, *108*, 13177–13184.
37. de Gennes, P.-G.; Brochard-Wyart, F.; Quéré, D. *Capillarity and Wetting Phenomena: Drops, Bubbles, Pearls, Waves*; Springer: New York, 2004.
38. Liu, H.; Tao, G. H.; Evans, D. G.; Kou, Y. Solubility of C_{60} in Ionic Liquids. *Carbon* **2005**, *43*, 1782–1785.
39. Matsumoto, Y.; Obata, T.; Hiraoka, M.; Katayama, M. Development of Variable Temperature UHV-laser Microscope Combined with Pulsed Laser Deposition for *In Situ* Studies on Ceramics/Metallic Glass Interfaces. *Ceram. Trans.* **2007**, *198*, 15–20.